Dependence of Raman frequencies and scattering intensities on pressure in GaSb, InAs, and InSb semiconductors

K. Aoki,* E. Anastassakis,† and M. Cardona
Max-Planck-Institut für Festkörperforschung, Heisenbergstrasse 1, D-7000 Stuttgart 80, Federal Republic of Germany
(Received 27 January 1984; revised manuscript received 26 March 1984)

The first-order Raman scattering by TO and LO phonons has been measured in GaSb, InAs, and InSb under hydrostatic pressures up to their phase transitions. The Raman frequencies increase nearly linearly while the LO-TO splitting decreases with increasing pressure. The scattering intensities display strong enhancement as the E_1 band gaps approach the laser frequencies with increasing pressure. The measured volume dependence of the Raman frequencies and the transverse effective charges is interpreted by means of pseudopotential calculations. The resonance behavior is discussed in terms of resonant Raman scattering near the E_1 gaps.

I. INTRODUCTION

Raman scattering is a powerful technique for studying the anharmonic behavior of solids under pressure. First- and second-order Raman scattering by phonons has been measured for a number of materials at pressures above 10 GPa following the development of the diamond anvil cell.[1] For zinc-blende–type compounds, the measurement of the phonon frequencies over a wide pressure range is particularly interesting. In addition to the mode Grüneisen parameters γ, the transverse effective charge e_T^* can also be obtained as a function of volume from the measured TO- and LO-phonon frequencies.[2–4] This effective charge can be taken as a measure of the ionicity of these compounds. Raman scattering also yields data on the semiconductor-metal transition of these materials at very high pressures.

Linear or nearly linear shifts of Raman frequencies with lattice constant have been found in a number of III-V compounds.[1–4] A precise measurement of the LO-TO splitting for GaAs, InP (Ref. 2), SiC (Ref. 3), AlN, BN, and BP (Ref. 4) has revealed that all compounds except SiC show a decrease of $|e_T^*|$ with decreasing bond length. A quantitative interpretation of the observed results was made using bond-orbital theory and also pseudopotential calculations of the effective charge.[2–4] These compounds have rather large optical gaps in the visible region at normal and/or high pressures. Thus, it is possible to measure the Raman spectra (versus pressure) of the compounds with laser lines in the transparency region, a fact which yields large scattering intensities.

In this paper we present similar data for the small-band-gap III-V semiconductors GaSb, InAs, and InSb. Phase transitions from semiconductor to metal were observed at 7.65±0.10, 7.60±0.15, and 3.10±0.10 GPa for GaSb, InAs, and InSb, respectively. The measured Raman frequency shifts are interpreted by means of pseudopotential calculations. The dependence of e_T^* on lattice constant is discussed in terms of the semiempirical bond-orbital model and the pseudopotential theory of the dynamical charge. The pressure dependence of the Raman scattering intensities taken for a fixed laser line is compared with resonance Raman scattering measurements at atmospheric pressure near the E_1 gaps.

II. EXPERIMENT

The measurements were carried out with a diamond cell designed by Syassen and Holzapfel.[5] The pressure was determined from the shifts of the ruby fluorescence lines.[6] Raman scattering by the TO and LO phonons from a polished (111) face was measured simultaneously in the back-scattering configuration. For InSb, the scattering by TO phonons from the (110) face and by LO phonons from the (100) face was also measured since the weak peak intensities and the small LO-TO splitting made it difficult to separate the two peaks when obtained simultaneously from a (111) face. The 5309-Å (2.335-eV), 4680-Å (2.650-eV), and 5682-Å (2.182-eV) lines of a Kr^+-ion laser were used for the measurements of GaSb, InAs, and InSb, respectively. These exciting lines have energies about 100 meV above the corresponding E_1 gaps. The Raman spectra were taken with a Spex double monochromator and an RCA-31034 photomultiplier in a photon-counting mode. All measurements were made at room temperature.

III. RESULTS

Figure 1 shows Raman spectra of GaSb taken for the 5309-Å line at various pressures. With increasing pressure, the LO and TO phonons shift to higher frequencies and their peak heights also vary: These phonons increase with increasing pressure in the low-pressure region, go through a maximum, and then decrease. The Raman frequencies of InAs and InSb also increased with increasing pressure. Similar changes in scattering intensity were found in InAs for the 4680-Å line, while InSb showed no significant peak-height change with pressure for the 5682-Å line.

The transition into the metallic phase occurred at 7.65±0.10 GPa in GaSb, 7.60±0.15 GPa in InAs, and 3.10±0.10 GPa in InSb. The transition pressure for GaSb was within the range of earlier data which range between 6.7 and 8.4 GPa,[7] but differed considerably from the

 ©1984 The American Physical Society

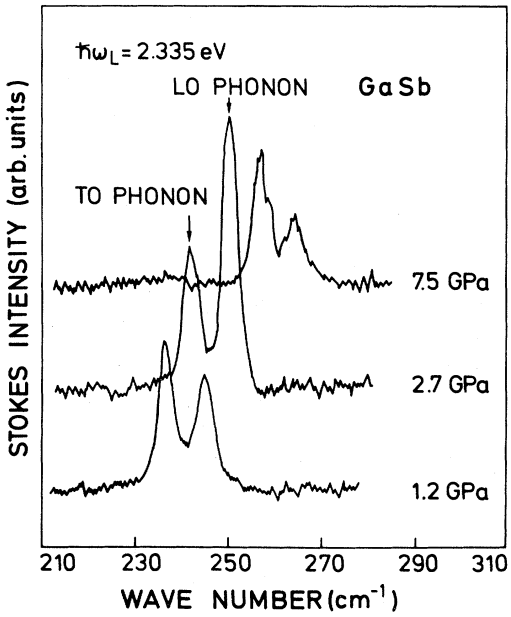

FIG. 1. First-order Stokes Raman spectra for GaSb taken with the 5309-Å laser line at different pressures.

latest value obtained by Yu *et al.*[8] by x-ray diffraction: These authors found a transition to the β-Sn structure at 6.2±0.3 GPa. The transition pressure found by us for InAs lies between the value of Minomura and Drickamer[7] (8.4 GPa) and that of Pitt and Vyas[9] (6.9 GPa). Our value for InSb is in good agreement with earlier results[10,11] (3.0 GPa).

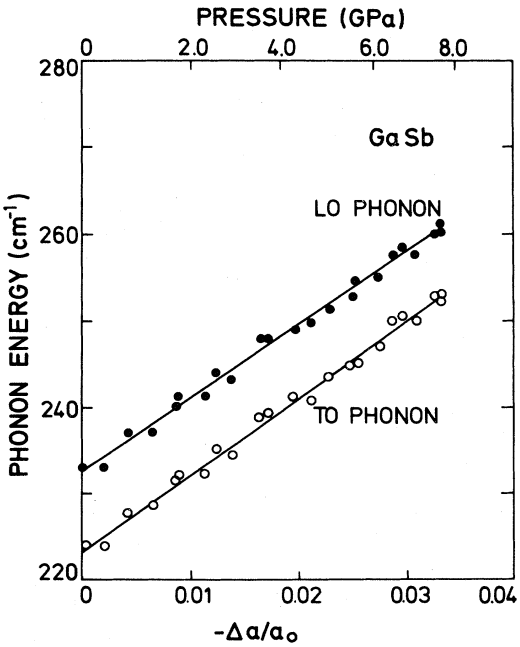

FIG. 2. Dependence of the TO- and LO-phonon frequencies of GaSb on linear lattice compression (lower scale) and pressure (upper scale). Solid lines are least-squares fits to the experimental data.

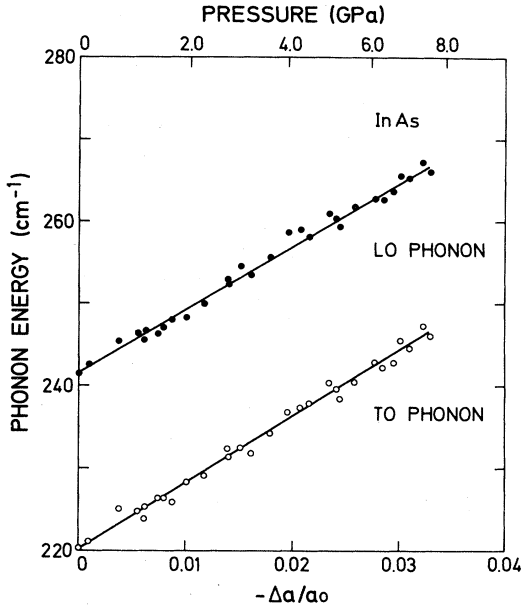

FIG. 3. Same results as in Fig. 2 but for InAs.

The shifts of the TO- and LO-phonon frequencies with relative lattice constant, $-\Delta a/a_0$ (lower scale) and pressure (upper scale) are given in Figs. 2–4. The measured pressures were converted to lattice constants by using Murnaghan's equation[12]

$$P=(B_0/B_0')[(a_0/a)^{3B_0'}-1]\,, \tag{1}$$

where B_0 is the bulk modulus and B_0' its pressure derivative. The following values of B_0 and B_0' were used: 58.9 GPa and 4.75 for GaSb,[13] 57.9 GPa and 4.79 for InAs,[14] and 45.7 GPa and 4.89 for InSb,[15] respectively. The observed frequencies, ω_{TO} and ω_{LO}, show sublinear depen-

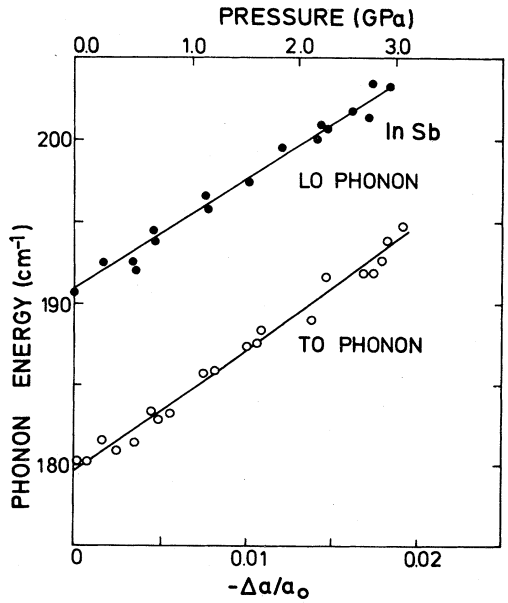

FIG. 4. Same results as in Fig. 2 but for InSb.

dence on pressure but nearly linear dependence on lattice constant. The experimental points were fitted to quadratic expressions in p and also in $\Delta a/a_0$. The results of these fits are

$$\omega_{TO}^{GaSb}=223.6(3)+4.67(13)P-0.11(2)P^2$$
$$=223.6(3)-863(30)(\Delta a/a)\,, \quad (2)$$
$$\omega_{LO}^{GaSb}=232.6(3)+4.56(13)P-0.12(2)P^2$$
$$=232.6(3)-842(30)(\Delta a/a)\,,$$
$$\omega_{TO}^{InAs}=220.4(3)+4.39(13)P-0.11(2)P^2$$
$$=220.4(3)-800(40)(\Delta a/a)\,, \quad (3)$$
$$\omega_{LO}^{InAs}=241.1(3)+4.57(13)P-0.15(2)P^2$$
$$=241.1(3)-769(40)(\Delta a/a)\,,$$
$$\omega_{TO}^{InSb}=179.7(3)+5.01(17)P-0.10(5)P^2$$
$$=179.7(3)-761(25)(\Delta a/a)\,, \quad (4)$$
$$\omega_{LO}^{InSb}=190.7(3)+5.11(25)P-0.31(8)P^2$$
$$=190.7(3)-668(37)(\Delta a/a)\,,$$

with ω in cm^{-1} and P in GPa.

Born's transverse dynamic charge e_T^* (Ref. 16) was evaluated from the relation between e_T^* and the $\omega_{LO}-\omega_{TO}$ splitting using

$$e_T^{*2}=(\Omega M/4\pi)\epsilon_\infty(\omega_{LO}^2-\omega_{TO}^2)\,, \quad (5)$$

where Ω is the volume of the unit cell, M is the reduced mass, and ϵ_∞ is the infrared dielectric constant. Although there are no experimental data for the volume dependence of ϵ_∞, we can reasonably assume $d\ln\epsilon_\infty/d\ln a\simeq 3$ according to the discussion in Ref. 2. The dependence of e_T^* on lattice constant obtained from Eq. (5) under this assumption is shown by the points of Figs. 5–7. The results are similar to those found for GaAs and InP.[2] The effective charge decreases with decreasing lattice constant. A possible quadratic term in this dependence, found for GaAs and InP,[2] is difficult to discern within the small pressure range available in these materials before the phase transition occurs. Thus in Figs. 5–7, we only show the linear fits.

Figure 8 displays the variation of the Raman scattering intensity (i.e., peak height; we did not notice any change in linewidth with pressure) in GaSb with pressure (lower scale) and the corresponding E_1 gap energy (upper scale). The data have not been corrected for absorption of the incident and scattered radiation. The E_1 gap at a pressure P was evaluated from the relation

$$E_1\ (\text{eV})=2.03+0.065(5)P\,,$$

which was found by means of reflectivity measurements up to 1 GPa.[17] The resonance behavior is clearly seen in both TO and LO phonons. As the E_1 gap approaches the incident photon energy with increasing pressure, the scattering intensity is resonantly enhanced. The resonance peak occurs at 3.2 GPa. The corresponding E_1 energy is 2.240 eV, smaller by about 0.1 eV than the incident photon energy of 2.335 eV.

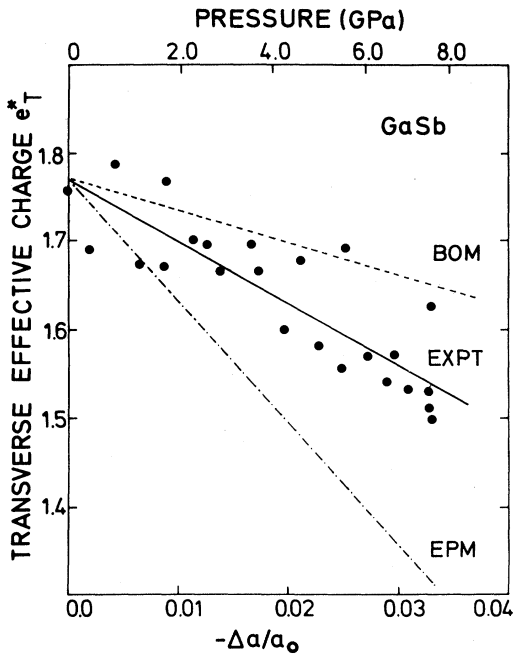

FIG. 5. The transverse effective charge e_T^* as a function of lattice compression (lower scale) and pressure (upper scale) for GaSb. The points, which are fitted by the solid line, were obtained from the measured pressure dependence of the TO- and LO-phonon frequencies of Fig. 2 and with the use of Eq. (5). Dashed and dot-dashed lines represent theoretical estimates as indicated. The calculated results are shifted vertically so as to fit the experimental results at normal pressure.

Figure 9 shows similar data for InAs taken with the 4680-Å line. The E_1 gap of InAs has an energy of 2.49 eV at normal pressure and increases with pressure at the

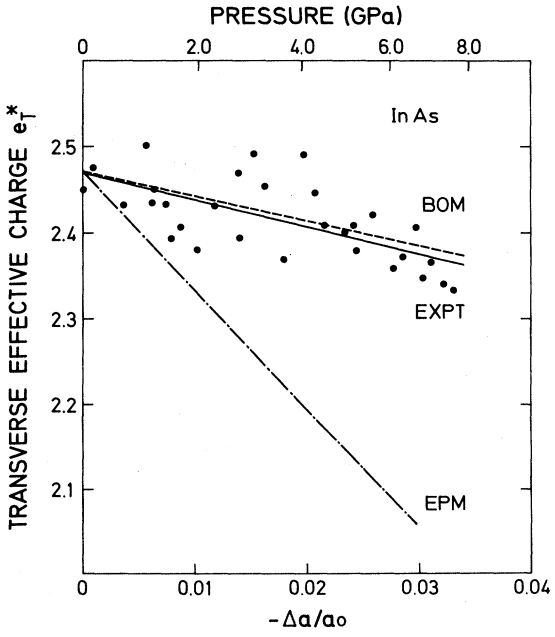

FIG. 6. Same results as in Fig. 5 but for InAs.

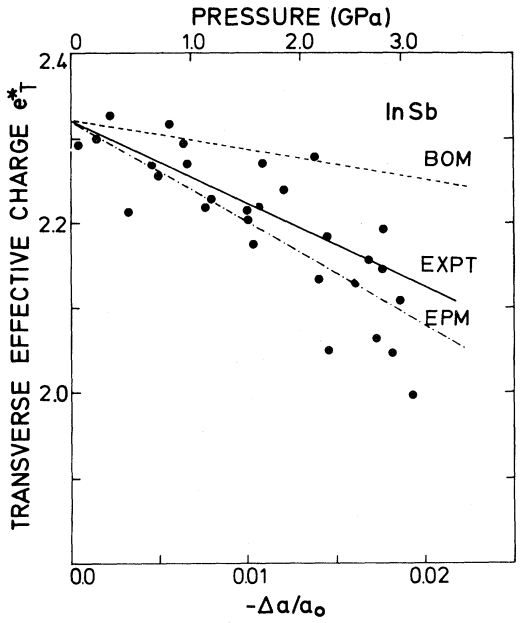

FIG. 7. Same results as in Fig. 5 but for InSb.

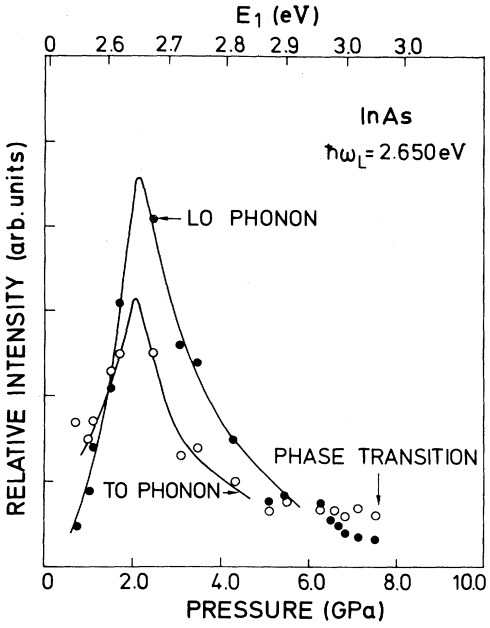

FIG. 9. Same as Fig. 8 but for InAs measured with the 4680-Å line. Solid lines are from Refs. 23–25.

rate of 0.074(5) eV/GPa.[17] Rather sharp resonance peaks were obtained. The asymmetric shape of the peaks can be attributed to strong absorption of the incident and scattered radiation on the low-pressure side of the peak. The E_1 gap is still below the incident photon energy in that pressure region. The resonance peak occurs at 2.2 GPa, where the E_1 gap has the same energy as that of the incident photon. No resonance enhancement was observed in InSb for the 5682-Å line: Obviously, the E_1 gap did not reach the incident photon energy even at the transition pressure.

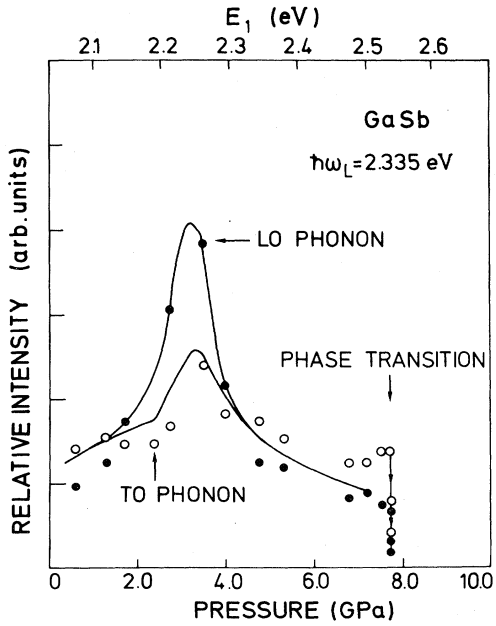

FIG. 8. Pressure dependence of the TO- and LO-phonon scattering from a (111) face for GaSb measured with the 5309-Å line. Upper scale indicates the estimated E_1 gap at the corresponding pressure. Solid lines show the spectral dependence of allowed TO- and LO-phonon scattering as reported in Ref. 22. The experimental data have not been corrected for absorption.

IV. DISCUSSION

The Raman frequencies of GaSb, InAs, and InSb shift nearly linearly with lattice constant. This linearity is a common characteristic of zinc-blende–type III-V compounds in spite of the wide range of electronic properties, from large-gap insulators such as BN to small-gap semiconductors such as InSb. In order to interpret the observed frequency shifts, the Raman phonon frequencies were calculated as a function of the lattice constant a by means of pseudopotential theory.[18] This microscopic method yields the following simple and intuitive approximate expression for the TO frequencies at Γ (in a.u.):

$$\omega_{\mathrm{TO}}^2=(M\Omega)^{-1}(4\pi Z_1 Z_2/3-E)\,, \tag{6}$$

$$E=(\Omega^2/12)\sum_{|\vec{G}|\neq\vec{0}} S(G)G^2[V_S^2(G)-V_A^2(G)] \times(G^2/4\pi e^2)\epsilon_G(1-\epsilon_G)\,, \tag{7}$$

$$S(G)=\sum_{\text{star of }\vec{G}} \exp[i\vec{G}\cdot(\vec{X}_2-\vec{X}_1)]\,, \tag{8}$$

where M is the reduced mass of the primitive cell, Ω is the volume of this cell, $\vec{X}_1$ and $\vec{X}_2$ are the ion positions in this cell, Z_1 and Z_2 are the ion-core charges (for III-V compounds $Z_1=3$ and $Z_2=5$), $V_S(G)$ and $V_A(G)$ are the symmetric and antisymmetric pseudopotential form factors,[19] $\vec{G}$ the reciprocal-lattice vectors, and ϵ_G is the G-

dependent dielectric function for $\omega=0$.[20] The first term in the right-hand side of Eq. (6) is the ionic plasma frequency contribution $4\pi Z_1 Z_2/3M\Omega$, and is related to the force due to the Coulomb field of the displaced ion core. The second term is the electronic contribution E. It is related to the force due to the potential setup by the valence electrons which are redistributed by the displacement of the cores.

For the purpose of the numerical calculation, the expression[19]

$$V(G)=\frac{8\pi Z}{G^2\epsilon_G}\frac{\cos(\vec{G}\cdot\vec{R})}{\Omega} \tag{9}$$

was used for $V(G)$ in Eq. (7). The core radius R employed in this work was 1.054 for Ga, 1.001 for Sb, 1.098 for In, and 0.952 for As (in Bohr units).[19] The main contribution of E to $\omega_{\rm TO}^2$ comes from $\vec{G}(200)$: For the star of $\vec{G}(111)$, the structure factor $S(G)$ is 0.[18] The stars of larger reciprocal-lattice vectors can be neglected since the higher pseudopotential Fourier coefficients converge rather rapidly. Therefore, only the $\vec{G}\{200\}$ star was taken into account.

The calculated Raman frequencies at normal pressure are given in Table I. The calculated TO frequencies are within 10% of the experimental values. The ionic contribution $4\pi Z_1 Z_2/3$ to $\omega_{\rm TO}^2$ is 62.83, while the electronic contribution E is found to be around 26 for GaSb, InAs, and InSb. GaP, a semiconductor with a rather large gap, has a similar value of E, namely 25.5. These results show that the magnitude of the electronic contribution is nearly the same in all III-V compounds in spite of the wide range of electronic properties. The smaller-gap semiconductors have lower Raman frequencies. This trend is easily attributed to the larger mass and unit-cell volume in these materials. Neither the larger optical dielectric constant nor the smaller energy gap directly imply a softening of the phonons.

The effect of volume on $\omega_{\rm TO}$ appears through the electronic contribution E. This term contains several factors depending on volume, but none of these factors dominates. A few percent changes in $G(200)$, $V_S(G)$, $V_A(G)$, and ϵ_G accumulate to a 10% change in E for a 2% decrease in a. The electronic contribution decreases with lattice compression, while the ionic contribution remains constant. $\omega_{\rm TO}^2$ is proportional to the difference between these two terms. Consequently, the decrease of E with lattice compression causes shifts to a higher frequency.

Mode Grüneisen parameters were calculated with this pseudopotential model for the zinc-blende–type III-V compounds measured. The experimental and calculated results are summarized in columns 1–3 of Table II. This model gives $\gamma_{\rm TO}=1.0$ to 1.2 for all III-V compounds and shows a slight increase with increasing reduced mass. The experimental values of γ are somewhat larger than the calculated values, ranging from 1.09 to 1.6. No systematic change or chemical trend is found.

Two different approaches to calculating the transverse effective charge e_T^* and its volume dependence have been suggested. The first approach is based on the pseudopotential method, the other approach is based on the semiempirical bond-orbital model for the tetrahedral semiconductors. The detailed expression and results of the full pseudopotential calculation have been presented in Refs. 2–4. In this work we adopt a simple algebraic expression for e_T^*,[2] where only two pseudopotential form factors at $G(111)$ and $G(200)$, labeled $V_\alpha(3)$ and $V_\alpha(8)$ ($\alpha=1$ for cation and $\alpha=2$ for anion), appear:[2]

$$\begin{aligned} e_T^* &= -\Delta Z-(8/E_g)[V_A(8)+2V_S(3)V_A(3)/E_x]\,, \\ E_g &= V_1(8)+V_2(8)+(1/E_x)[V_1^2(3)+V_2^2(3)]\,, \\ E_x &= \tfrac{1}{2}(2\pi/a)^2\,. \end{aligned} \tag{10}$$

The notation in Eq. (10) is that of Eqs. (6)–(8). The model pseudopotential of Eq. (9) was also used for the numerical calculation of the dependence of e_T^* on volume. Within the bond-orbital model,[21] the effective charge is expressed as a function of polarity α_P,

$$e_T^*=-\Delta Z+\tfrac{20}{3}\alpha_P-\tfrac{8}{3}\alpha_P^3\,, \tag{11}$$

where the polarity α_P is written

$$\alpha_P=V_3(V_2^2+V_3^2)^{-1/2}\,. \tag{12}$$

In Eq. (12), V_2 represents a covalent energy gap related to the overlap between atomic orbitals on adjacent atoms, and V_3 is an ionic contribution to the gap defined by one half of the energy difference between anion and cation. According to this model, the covalent term V_2 varies with lattice constant a as a^{-2}, while the ionic term V_3 can be assumed to be independent of a. Thus, this model gives a straightforward procedure to calculate e_T^* versus a. The results are represented by dashed lines in Figs. 5–7.

The experimental and calculated results for e_T^* are summarized in columns 4–9 of Table II. The values of e_T^* obtained with the bond-orbital model are in good agreement with the experimental values for all III-V compounds except for BP. For GaSb, InAs, and InSb, the

TABLE I. Observed and calculated Raman frequencies for GaSb, InAs, and InSb. Ionic and electronic contributions to $\omega_{\rm TO}^2$ obtained with the pseudopotential calculation of Eqs. (6)–(8) are given in the fourth and fifth columns, respectively.

	$\omega_{\rm TO}$ (obs) ($\rm cm^{-1}$)	$\omega_{\rm LO}$ (obs) ($\rm cm^{-1}$)	$\omega_{\rm TO}$ (calc) ($\rm cm^{-1}$)	$\frac{4}{3}\pi Z_1 Z_2$	E
GaSb	223.6	232.6	244.9	62.83	24.4
InAs	220.4	241.1	248.3	62.83	23.2
InSb	179.7	190.7	179.9	62.83	29.6

TABLE II. Mode Grüneisen parameters of the zone-center phonons, and the transverse effective charge and its dependence on lattice constant as measured experimentally and as calculated with various pseudopotential approaches [Eqs. (6) and (10)] and with the bond-orbital model (BOM) [Eq. (11)] for III-V compounds.

				e_T^*			$\frac{\partial e_T^*}{\partial \ln a_0}$		
	γ_{TO} (expt)	γ_{LO} (expt)	γ_{TO} (calc)	Expt	Pseudopotential	BOM	Expt	Pseudopotential[a]	BOM
BN[a]	1.5	1.2		1.98	2.78[b]	1.17	1.61	4	3.45
BP[a]	1.3	1.12	1.00	−1.34	−1.38[b]	0.31	10	2	2.44
AlN[a]	1.6	1.0		2.57	2.91[b]	2.36	5	1	3.06
GaP	1.09[c]	0.95[c]	1.05	2.04[c]	2.11[b]	2.05	3[c]	8.8	3.46
GaAs[d]	1.39	1.23	1.09	2.16[d]	1.71[b]	1.86	4.4	8.3	3.59
GaSb	1.33	1.21	1.16	1.74	5.11	1.73	6.7	12.8	3.63
					1.86[e]			7.0[b]	
InP[d]	1.44	1.24	1.19	2.55[d]	1.81	2.35	4.5	8.5	3.06
InAs	1.21	1.06	1.18	2.45	4.49	2.26	3.3	14.3	3.21
					1.69[e]			14.6[b]	
InSb	1.41	1.17	1.19	2.28	5.36	2.10	9.7	11.7	3.42
					2.16[e]			7.6[b]	

[a]From Ref. 4.
[b]Full pseudopotential calculations, see Ref. 4.
[c]From Ref. 1.
[d]From Ref. 2
[e]Full pseudopotential calculation, P. Vogl (unpublished).

simple pseudopotential theory gives much larger values, a fact probably due to the oversimplifications involved in Eq. (10). The full pseudopotential calculations for other III-V compounds[4] yielded nearly correct values as given in Table II.

The dependence of e_T^* on lattice constant shows a similar trend. The pseudopotential calculation yields a stronger volume dependence than those observed experimentally, while the bond-orbital calculation yields a weaker dependence, a fact which is common to all III-V compounds except for the larger band-gap materials (BN, BP, and AlN) (see dashed and dot-dashed lines in Figs. 5—7).

Next, we discuss the dependence of the scattering intensity on pressure. The peak of the scattering intensity observed in GaSb and InAs is interpreted as a resonance phenomenon. Resonance Raman scattering near the E_1 and $E_1+\Delta_1$ gaps has been studied for GaSb by Dreybrodt *et al.*,[22] and for InAs by Leite and Scott,[23] Rubloff *et al.*,[24] and Renucci *et al.*[25] These authors found a strong enhancement of the allowed scattering by TO and LO phonons for laser photon energies near the E_1 gaps. Forbidden scattering due to Fröhlich interaction is also seen for LO phonons, especially near resonances and at low temperatures. At room temperature, however, the forbidden LO scattering seems to be small compared with its allowed counterpart.[25] Hence, we interpret the results of Figs. 8 and 9 as due to *allowed* resonant scattering. The allowed Raman scattering efficiency can be written as[22]

$$S \propto \left| A\frac{d\chi}{d\omega} + B(\chi^+ - \chi^-) + C \right|^2 , \tag{13}$$

where χ represents the susceptibility tensor, and χ^+ and χ^- are the contributions to this tensor which result from the E_1 and $E_1+\Delta_1$ gaps. The relative contributions of the three terms in Eq. (13) to the Raman tensor are determined by the coefficients A, B, and C. By using experimental data for the dielectric constant, a spectral distribution of the Raman efficiency is obtained. The calculated resonance shapes for the TO and LO phonons of GaSb have shown reasonably good agreement with the observed resonance shapes after the absorption correction.[22]

The pressure dependence of the scattering intensity arises from the pressure dependence of the gaps which in turn, induces a pressure dependence of χ. For diamond-type and zinc-blende—type semiconductors, the E_1 and $E_1+\Delta_1$ gaps increase with increasing pressure. There are no data for the pressure dependence of the dielectric constants of GaSb and InAs, and in particular there are no data near E_1 and $E_1+\Delta_1$. One can, however, assume that the effect of pressure on χ is mainly to shift the E_1 and $E_1+\Delta_1$ singularities to higher photon energy with little change in the shape of χ.[26] This assumption enables us to treat equivalently the two types of resonance, that obtained by tuning the energy of the incident light through fixed E_1 and $E_1+\Delta_1$ gaps (constant pressure) and that found by tuning the E_1 and $E_1+\Delta_1$ gaps while changing the pressure for a fixed incident photon energy.

The comparison between the two resonances is made for GaSb using the raw data without the absorption correction in Fig. 8. The solid lines represent the spectral dependence of the scattering cross sections for allowed TO and LO phonons obtained at room temperature.[22] The peak positions were fitted to those of the high-pressure data. The agreement of both resonant profiles is quite good. Note that the resonance peak near the E_1 gap occurs at an energy $\hbar\omega_L \sim 0.1$ eV higher than that of the

corresponding gap. This apparent anomaly occurs for both the resonance as a function of $\hbar\omega_L$ and also the resonance as a function of pressure keeping $\hbar\omega_L$ constant. It may be a result of the complicated structure of Eq. (13) in which the peak maximum need not correspond to the critical energy E_1. Unfortunately, the available Raman and χ data are not sufficiently detailed to allow a clarification of this point.

A similar comparison is made for InAs in Fig. 9. The solid lines represent the spectral resonance data for allowed TO and LO phonons at room temperature obtained by combining the data of Refs. 23–25. Again, good agreement is obtained between the two resonance peaks. The full width of the resonance at half maximum is about 0.1 eV for both TO and LO phonons. The resonance peaks obtained in the measurements under pressure show asymmetric shapes, rising more sharply from the nonresonance background level on the low-pressure side. The lower intensity on the low-pressure side of the resonance peak seems to be due to absorption of the incident and scattered light. In the low-pressure region, the E_1 gap is still below the incident photon energy: The larger absorption coefficient produces a smaller scattering volume. Similarly, an asymmetric peak due to absorption is found in the spectral resonance data at constant pressure if the absorption correction is not performed. The estimated E_1 gap under exact resonance conditions has nearly the same energy as the incident photon, $\hbar\omega_L = 2.650$ eV. On the other hand, the spectral resonance data taken at normal pressure shows that the resonance peak occurs at 2.60 eV, about 0.10 eV above the E_1 optical gap. This discrepancy may be attributed to an overestimate of the pressure coefficient of the E_1 gap. Note that the pressure coefficient given in Ref. 17 for the E_1 gap is 0.074(10) eV/GPa. In principle this coefficient should be nearly the same as that of the $E_1+\Delta_1$ gap [0.063(10) eV/GPa].

The sharp resonance peaks in Figs. 8 and 9 for GaSb and InAs were obtained for fixed laser lines by tuning the E_1 gaps with pressure. The position of the resonance peaks was determined to an accuracy of ± 0.2 GPa, which corresponds to an accuracy of ± 0.014 eV for the E_1 gap. These experimental results suggest that it should be possible to determine the dependence of the E_1 gaps on pressure by carrying out successive resonance measurements under pressure for several different laser lines. In contrast to the E_0 gaps, the E_1 gaps have been measured only up to rather low pressures (below 1 GPa) by means of reflectivity measurements.[17] The resonance Raman scattering technique easily extends the pressure range for which measurements are possible to pressures above 10 GPa. If such measurements were also to become possible for the $E_1+\Delta_1$ gap they would yield valuable information on the pressure dependence of the spin-orbit splitting Δ_1, of which little information is available.[27]

ACKNOWLEDGMENTS

Thanks are due to Dr. P. Vogl for making his pseudopotential results available to us prior to publication. We also thank H. Hirt, M. Siemers, and P. Wurster for technical assistance and to A. Jayaraman for supplying his data for InAs (prior to publication), which are in basic agreement with those reported here.

*Permanent address: National Chemical Laboratory for Industry, Yatabe, Ibaraki 305, Japan.

†Permanent address: Department of Physics, Technical University of Athens, Athens, Greece.

[1]B. A. Weinstein and R. Zallen, in *Light Scattering in Solids IV*, edited by M. Cardona and G. Güntherodt (Springer, Heidelberg, 1984).

[2]R. Trommer, H. Müller, M. Cardona, and P. Vogl, Phys. Rev. B **21**, 4869 (1980).

[3]D. Olego, M. Cardona, and P. Vogl, Phys. Rev. B **25**, 3878 (1982).

[4]J. A. Sanjurjo, E. López-Cruz, P. Vogl, and M. Cardona, Phys. Rev. B **28**, 4579 (1983).

[5]K. Syassen and W. Holzapfel, Phys. Rev. B **18**, 5826 (1978).

[6]J. D. Barnett, S. Block, and G. J. Piermarini, Rev. Sci. Instrum. **44**, 1 (1973); G. J. Piermarini, S. Block, J. D. Barnett, and R. A. Forman, J. Appl. Phys. **46**, 2774 (1975).

[7]S. Minomura and H. G. Drickamer, J. Phys. Chem. Solids **23**, 451 (1962).

[8]S. C. Yu, I. L. Spain, and E. F. Skelton, Solid State Commun. **25**, 49 (1978).

[9]G. D. Pitt and M. K. R. Vyas, J. Phys. C **6**, 274 (1973).

[10]B. Okai and J. Yoshimoto, J. Phys. Soc. Jpn. **45**, 1880 (1978).

[11]D. R. Yoder-Short, R. Colella, and B. A. Weinstein, Phys. Rev. Lett. **49**, 1438 (1982).

[12]F. D. Murnaghan, Proc. Natl. Acad. Sci. U.S.A. **30**, 244 (1944).

[13]H. J. McSkimin, A. Jayaraman, P. Andreatch, and T. B. Bateman, J. Appl. Phys. **39**, 4127 (1968).

[14]M. R. Vukcevich, Phys. Status Solidi B **54**, 219 (1972).

[15]I. O. Bashkin and G. I. Peresada, Sov. Phys. Solid State **16**, 2058 (1975).

[16]M. Born and K. Huang, *Dynamical Theory of Crystal Lattices* (Clarendon, Oxford, 1954), Chap. 2.

[17]R. Zallen and W. Paul, Phys. Rev. **155**, 703 (1967).

[18]W. Porod, P. Vogl, and G. Bauer, J. Phys. Soc. Jpn. Suppl. **49**, A649 (1980).

[19]M. L. Cohen and V. Heine, in *Solid State Physics*, edited by H. Ehrenreich, F. Seitz, and D. Turnbull (Academic, New York, 1970), Vol. 24, p. 37.

[20]D. Penn, Phys. Rev. **128**, 2093 (1962).

[21]W. A. Harrison and S. Ciraci, Phys. Rev. B **10**, 1516 (1974).

[22]W. Dreybrodt, W. Richter, F. Cerdeira, and M. Cardona, Phys. Status Solidi B **60**, 145 (1973); F. Cerdeira, W. Dreybrodt, and M. Cardona, in *Proceedings of the 11th International Conference on the Physics of Semiconductors* (PWN-Polish Scientific, Warsaw, 1972), Vol. 2, p. 1142.

[23]R. C. C. Leite and J. F. Scott, Phys. Rev. Lett. **22**, 130 (1969).

[24]G. W. Rubloff, E. Anastassakis, and F. H. Pollak, Solid State Commun. **13**, 1755 (1973).

[25]M. A. Renucci, J. B. Renucci, and M. Cardona, Phys. Status Solidi B **49**, 625 (1972); J. B. Renucci, M. A. Renucci, and M. Cardona, Solid State Commun. **9**, 1235 (1971).

[26]M. Cardona, in *Atomic Structure and Properties of Solids*, edited by E. Burstein (Academic, New York, 1972), p. 514.

[27]F. Cerdeira, J. de Witt, U. Rössler, and M. Cardona, Phys. Status Solidi **41**, 735 (1970).